2

SUBSONIC FINITE ELEMENTS FOR WING-BODY COMBINATIONS

James L. Thomas
NASA Langley Research Center

SUMMARY

Capabilities, limitations, and applications of various theories for the prediction of wing-body aerodynamics are reviewed. The methods range from approximate planar representations applicable in preliminary design to surface singularity approaches applicable in the later stages of detail design. The available methods for three-dimensional configurations are limited as inviscid solutions with viscous effects included on an empirical or strip basis.

INTRODUCTION

Current research efforts directed toward the design of fuel-efficient aircraft dictate that adequate tools be available for the assessment of aerodynamic loads across the expected speed envelope. Ashley and Rodden (ref. 1) have summarized the available methods for aerodynamic analyses of wings and bodies in steady and oscillatory motion at both subsonic and supersonic speeds. The analytical methods applicable to generalized configurations vary over a range of sophistication, accuracy, and computer times required but are generally limited as inviscid solutions. Some inviscid-viscid coupling techniques in two dimensions have yielded good results (refs. 2 and 3), and their inclusion on a strip basis into three-dimensional inviscid solutions may serve as a near-term solution. The inclusion of viscous effects for generalized configurations across the Mach number range remains a far-term solution requiring extensive computer resources and advances in turbulence modeling (ref. 4). Immediate design and verification methods are thus a combination of experimental and analytical techniques. The analytical methods largely remain inviscid solutions guided by the inclusion of viscous effects on a semiempirical or strip basis.

The purpose of this paper is to summarize the capabilities and limitations of the existing methods for the steady subsonic analysis of wing-body combinations. Solutions to the linearized perturbation potential equation (Laplace's equation), with Mach number effects included by the Prandtl-Glauert transformation, are considered. Since the governing partial differential equation is linear, the solutions may be approximated by distributing a finite number of elemental solutions over the body and solving for their relative strengths by imposing proper boundary conditions; for example, the flow field must satisfy the tangential requirement on the body surface and the Kutta condition at subsonic trailing edges. Such finite-element solutions have proven to be most useful and versatile at subsonic as well as supersonic speeds. The quality of the resulting solution is, however, a function of the type, distribution, and number of elemental solutions assumed. They require considerably less computer resources than the equivalent three-dimensional finite-difference solutions required at transonic speeds where the governing equations are nonlinear (ref. 5).

SYMBOLS

A	aspect ratio, b^2/S
b	wing span
C_L	lift coefficient
C_p	pressure coefficient
c	chord
c_l	section lift coefficient
d	body diameter
L	body length
M	Mach number
r	body radius
S	wing area
X,Y,Z	axis system
x,z	distances along X- and Z-axes
α	angle of attack
η	distance along semispan
Λ	sweep angle
λ	taper ratio

Subscripts:

av	average
max	maximum
∞	free stream
f	fuselage

GENERAL SLENDER BODY AND PLANAR WING SOLUTION

A large number of methods exist for the analysis of planar lifting surfaces which account approximately for the presence of bodies. Generally, the methods

treat the body separately in an initial analysis and then modify the analysis of the lifting surface such that the normal wash on the wing from the body is included and the flow is diverted around the body.

Slender body theory is used in the initial analysis of the body since its accuracy is consistent with the assumptions to be made in the wing-body interactions. Slender body theory assumes the total potential can be composed of a far-field potential dependent only on the area distribution and the Mach number and a near-field constant-density cross-flow potential solved subject to the three-dimensional boundary conditions of flow tangency at the surface (refs. 6 and 7). The equivalence rule extends the formulation to bodies of general cross section as indicated in figure 1. The flow around the actual body differs from that of the equivalent body of revolution by only a two-dimensional constant-density cross-flow potential that satisfies the flow tangency condition at the surface.

The constant-density cross-flow potential can be solved by any two-dimensional method. Dillenius, Goodwin, and Nielsen (ref. 8) have developed a solution applicable to noncircular fuselages composed of polar harmonic and two-dimensional source-sink terms. A conformal transformation and a distributed singularity approach are shown in figure 2. The conformal transformation is an adaption of the Theodorsen technique for airfoil design and was developed by Bonner of Rockwell International (ref. 9). The actual body is mapped into a circle and the potential for a source or doublet satisfying the boundary conditions for the equivalent body is transformed back to the physical plane. The method is very fast and simple but is limited to bodies in uniform flow fields that can be described in polar coordinates as a single-valued function of radius versus subtended angle. The distributed singularities approach was developed by J. Werner and A. R. Krenkel of Polytechnic Institute of New York and solves for the strengths of constant-strength source segments around the body by satisfying the flow tangency requirement. The method is applicable to very arbitrary bodies in nonuniform flow fields. Comparison of the conformal transformation technique of Bonner with experiment (ref. 10) for a parabolic body of revolution of fineness ratio 12 and elliptic cross section is shown in figure 3. The agreement at this high subsonic Mach number at angles of attack of 0° and 4° is generally very good.

Giesing, Kálmán, and Rodden (ref. 11) and Dillenius, Goodwin, and Nielsen (ref. 8) have developed methods based on general slender body theory in combination with vortex-lattice theory and the method of images. In both methods, the influence of the body on the lifting surface is accounted for by including the normal wash exterior to the body and then imaging the external singularities inside the body. Since the method of images is based on a two-dimensional analysis, it does not entirely negate the normal wash from the wing onto the body. Thus, the body loading in the nonuniform flow field of the lifting surface and image system must be recalculated to solve for this residual potential. The complete solution is an iterative process in which the continued interaction between the body and the lifting surface needs to be computed. However, reference 8 has indicated the method is strongly convergent and most of the effects are included after the first iteration. The method of images is very attractive in that no new unknowns are introduced into the solutions since the image strength and location are directly related to the external singularity strengths and the geometry of the body cross section.

An alternate approach has been used by Spangler, Mendenhall, and Dillenius (ref. 12) and Woodward (ref. 13) to approximately account for interference effects. In their analysis, interference panels are placed on constant-section stream tubes of the body. The normal wash from the body is included on the lifting surface exterior to the body and the interference panels exist to cancel the normal wash induced on the surface of the body. The net result is exactly the same as that using the method of images in that the initial influence of the body on the wing is included and the normal wash onto the body from the wing is negated. However, there are more equations to solve when the interference panels are used, although the region of influence of the wing on the body can generally be assumed to be within a couple of chord lengths of the wing root. A schematic of the utilization of general slender body theory with a traditional vortex-lattice system is shown in figure 4.

The methods of images (ref. 14) and interference paneling in combination with a vortex lattice are compared with an earlier modified Multhopp lifting-line approach (ref. 15) for a high-aspect-ratio wing-body combination in figure 5. Both the method of images and the method of interference panels give similar results and give lower results for the loadings than the earlier Multhopp results. Reference 11 has compared the method of images with the interference paneling used by Woodward and the agreement is excellent.

The assumption with either approach is that the flow field around the body in the presence of the wing is the same as that for the body alone. Thin-wing assumptions are used which do not account for the finite regions of intersection between a wing and a body or the longitudinal acceleration of flow over the body on the wing. Because of the singularities trailing downstream with either images or interference paneling in accounting for interference effects, the body representation is restricted to constant-section cylinders. The methods thus give identical results for equivalent positions of the wing above or below the midwing position as indicated in figure 6. The results presented are for a high-aspect-ratio wing-body combination using a vortex lattice with interference paneling.

A comparison of the theoretical and experimental (ref. 16) span loads for a wing-body combination is given in figure 7. All the theoretical methods overestimate the span loading because of the low Reynolds number of the experiment (0.3×10^6). The more approximate theories, however, agree well in the loading prediction with the more exact surface singularity representations, such as those of Labrujere (ref. 17) or Hess (ref. 18), and, in general, adequate predictions of lift and moment are possible with the approximate theories.

The assumptions of the methods which limit their applicability to generalized configurations also enhance their capability as a preliminary design tool. Most of the wing-body interactions are handled and the computer resources required are small because of the relatively small number of unknowns. Since planar representations are used, the intersection of the wing and body is a line and the geometry can be input rapidly. The capability is provided to predict quickly and accurately overall lift, moment, and induced drag for complete configurations at the early design stage, such as in the store separation studies of reference 8. The prediction of optimum trimmed loadings subject to lift and moment constraints are also possible from a far-field equivalent-horseshoe-vortex Trefftz plane analysis such as in references 19 and 20.

QUADRILATERAL VORTEX AND SOURCE LATTICE SOLUTION

A method which computes the interfering flow fields of both wing and body simultaneously while still retaining the linearized boundary condition is that of Tulinius (ref. 21). The method distributes a series of constant-strength quadrilateral vortices over the surface of the body and in the region of the wing near the wing-body intersection region as shown in figure 8. Horseshoe vortices are used in regions of the wing away from the wing-body intersection region. A source lattice is distributed over the surface of the wing at the quarter-chord and three-quarter-chord of each panel, and the source strengths are defined as the local slopes of the thickness distribution independent of the wing lift. The influence of the quadrilateral vortex dies off rapidly at points away from the quadrilateral because of the canceling effects of adjacent sides. Hence, the panels can be extended over the fore and aft regions of the body. The analysis has been extended to predict thick wing and pylon-fuselage-fanpod-nacelle characteristics at subsonic speeds by placing the vortices along the mean camber line of the wing (ref. 22).

Results of the Tulinius wing-body program are compared with experiment in figures 9, 10, and 11 for a swept wing-body combination at a Mach number of 0.60 and an angle of attack of 4°. The unit span load $c_l c/C_L c_{av}$ and the longitudinal distribution of fuselage lift $c_{l,f} d/d_{max}$ are predicted very well by the theory (fig. 9); the fuselage lift increases rapidly in the region of the wing root. The pressure coefficients on the wing at two spanwise stations in figure 10 and the pressure coefficients on the body at longitudinal stations just above and below the wing in figure 11 are also predicted well. The body pressures are influenced by the wing primarily in the wing root region, and the pressures over the aft end of the body are not predicted because of viscous and separation effects. The agreement with theory is expected since the wing is relatively thin and attached in the midwing position.

The method cannot account for the longitudinal acceleration of flow over the body on the wing (speed bump effect) or equivalent high and low positions of the wing because of the linearized planar boundary conditions. The pressure coefficients and not just loadings are predicted so that streamlining and contouring of adjacent surfaces at high subsonic Mach numbers can be accomplished. Regions of intersecting surfaces are lines so that geometry description is relatively easy. The number of equations to solve for the simultaneous quadrilateral and horseshoe vortex strength increases in comparison with the slender body and planar wing analyses but the quality of the aerodynamic solution is higher since the body and wing flow fields are solved simultaneously.

SURFACE SINGULARITY POTENTIAL FLOW

In order to account for the full potential interactions between the wing and body, a surface singularity technique such as that in references 17, 18, 23, 24, or 25 must be used. In such a method, the singularities are placed on the surface of the wing and body such that the tangency and Kutta conditions are satisfied. The type of finite-element modeling used for the lifting surfaces has been varied, including (1) constant-strength surface source panels with a constant-strength vortex sheet on the surface (ref. 18), (2) constant-strength

source panels on the surface with interior vortex sheet (ref. 17), or (3) linearly varying source and quadratically varying doublet distributions on curved surface panels (ref. 25). Constant-strength source panels have been generally used to model the body with the lifting surface carried through the body in order to approximately account for the wing carry-throug' 'ift.

Such a surface singularity approach accounts for the finite intersection region of a wing and body as well as the longitudinal velocity perturbations of the body on the wing. However, the method requires a considerable amount of geometry specification to panel a complete configuration as shown in figure 12. The quality of the resulting aerodynamic solutions are a function of the particular finite elements chosen, their placement on the body, and the number chosen. Since matrix solution times are a function of the number of elements cubed, the paneling of complete configurations with a minimum of computer time while retaining desired accuracy is a difficult task. Recent advances to relieve the dependence of the resulting solution on the aerodynamic paneling chosen and to reduce the number of unknowns required have been made in references 25 to 27.

Results for the Hess surface singularity approach (ref. 18) are presented in figure 13 for the $A = 6$ untapered unswept wing attached in intermediate, high, and low positions to an infinite circular-cylinder body - the case considered earlier with the approximate theory. The local span loading and total lift vary with the relative placement of the wing on the body; the body loads are shown as average values since the available version of the computer program only outputs pressures and integrated loads for the body. The intersection of the wing section with the curved body is another curved region that tends to accelerate the flow under the wing in a high wing position and above the wing in a low wing position. Since the singularities are on the surface, the local velocity increase on the lower surface of the high wing decreases the local loading and vice versa. Thus, the surface singularity approach yields differences in potential theory for high and low wing placement, whereas, the linearized planar lifting surface theories do not. However, the integrated values of lift differ very little with wing placement, indicating again that the approximate theories are able to give reasonable estimates of the total forces and moments.

The surface singularity approach is a detail design tool applicable in the later stages of design after the initial planform sizes and locations have been determined, such as in the design of cruise overwing nacelle configurations in reference 28. The inverse design for the surface singularity approach has been completed in reference 24, but the procedure for generalized configurations is necessarily lengthy and difficult. The surface singularity approach allows the calculation of detailed pressure distributions in regions of adjacent surfaces (wing fillets, nacelle-strut intersections, etc.) so that contouring and streamlining for minimum adverse pressure and viscous drag can be accomplished.

CONCLUDING REMARKS

Various approximate methods utilizing some variation of general slender body theory in combination with a planar lifting-surface representation, such as the vortex-lattice method or the constant-pressure panel of Woodward, are adequate to estimate the loads, moments, and pressures in preliminary design

applications. Such methods require limited computer resources and simple geometry input specifications and are well suited to inverse design procedures since the number of unknowns are small and the planar boundary conditions are retained. The methods are most applicable to midwing cases with constant-section cylindrical bodies.

An extension of the vortex-lattice method to include a quadrilateral vortex representation of the body solves for the wing and body loads simultaneously. No restrictions on body shape or wing shape in the intersection regions are made although the thin-wing representation is retained. Regions of intersecting surfaces are curved lines and the geometry input remains relatively simple. With the method, pressures in regions of adjacent surfaces are predicted to allow contouring and streamlining. The method is also well suited to inverse design procedures for the wing in the presence of the body since the camber and thickness solutions are separate.

In order to accurately predict the correct potential flow pressures in areas of intersecting wings and bodies, a surface singularity approach is needed. The surface singularity approach removes all thin-wing and linearized-boundary-condition assumptions but more than doubles the number of unknowns to be solved and the geometry definition required. The detail pressure distributions in regions of intersecting surfaces are available so that adverse viscous effects can be minimized.

Viscous effects are not predicted in any of the methods. For the present, empirical or strip analyses must be used, such as in the prediction of viscous effects using an infinite yawed-wing analogy in two-dimensional strips along a swept wing. The usefulness of all the wing-body theories depend on how well the theoretical loadings or pressures can be related to the actual physical situation. The nonlinear and viscous effects, such as vortex formation near the wing-body juncture or separated flow at higher angles of attack, remains untractable computationally. The viscous calculation for generalized configurations across the Mach number range remains a far-term solution.

REFERENCES

1. Ashley, Holt; and Rodden, William P.: Wing-Body Aerodynamic Interaction. Annual Review of Fluid Mechanics, Vol. 4, M. Van Dyke, W. G. Vincenti, and J. V. Wehausen, eds., Annual Rev., Inc., 1972, pp. 431-472.

2. Morgan, Harry L., Jr.: A Computer Program for the Analysis of Multielement Airfoils in Two-Dimensional Subsonic, Viscous Flow. Aerodynamic Analyses Requiring Advanced Computers, Part II, NASA SP-347, 1975, pp. 713-747.

3. Garabedian, Paul R.: Computational Transonics. Aerodynamic Analyses Requiring Advanced Computers, Part II, NASA SP-347, 1975, pp. 1269-1280.

4. Chapman, Dean R.; Mark, Hans; and Pirtle, Melvin W.: Computer vs. Wind Tunnels for Aerodynamic Flow Simulations. Astronaut. & Aeronaut., vol. 13, no. 4, Apr. 1975, pp. 22-35.

5. Bailey, F. R.; and Ballhaus, W. F.: Comparisons of Computed and Experimental Pressures for Transonic Flows About Isolated Wings and Wing-Fuselage Configurations. Aerodynamic Analyses Requiring Advanced Computers, Part II, NASA SP-347, 1975, pp. 1213-1231.

6. Adams, Mac C.; and Sears, W. R.: Slender Body Theory - Review and Extension. J. Aeronaut. Sci., vol. 20, no. 2, Feb. 1953, pp. 85-98.

7. Ashley, Holt; and Landahl, Marten: Aerodynamics of Wings and Bodies. Addison-Wesley Pub. Co., Inc., c.1965.

8. Dillenius, Marnix F. E.; Goodwin, Frederick K.; and Nielsen, Jack N.: Analytical Prediction of Store Separation Characteristics From Subsonic Aircraft. J. Aircr., vol. 12, no. 10, Oct. 1975, pp. 812-818.

9. Bonner, E.: Theoretical Prediction of Inviscid Three Dimensional Slender Body Flows. Report No. NA-74-687, Los Angeles Aircraft Div., Rockwell International Corp., 1974.

10. McDevitt, John B; and Taylor, Robert A.: Force and Pressure Measurements at Transonic Speeds for Several Bodies Having Elliptical Cross Sections. NACA TN 4362, 1958.

11. Giesing, J. P.; Kálmán, T. P.; and Rodden, W. P.: Subsonic Steady and Oscillatory Aerodynamics for Multiple Interfering Wings and Bodies. J. Aircr., vol. 9, no. 10, Oct. 1972, pp. 693-702.

12. Spangler, S. B.; Mendenhall, M. R.; and Dillenius, M. F. E.: Theoretical Investigation of Ducted Fan Interference for Transport-Type Aircraft. Analytic Methods in Aircraft Aerodynamics, NASA SP-228, 1970, pp. 703-719.

13. Woodward, Frank A.: Analysis and Design of Wing-Body Combinations at Subsonic and Supersonic Speeds. J. Aircr., vol. 5, no. 6, Nov.-Dec. 1968, pp. 528-534.

14. Giesing, Joseph P.: Lifting Surface Theory for Wing-Fuselage Combinations. Rep. DAC-67212, Vol. I, McDonnell Douglas, Aug. 1, 1968.

15. Weber, J.; Kirby, D. A.; and Kettle, D. J.: An Extension of Multhopp's Method of Calculating the Spanwise Loading of Wing-Fuselage Combinations. R. & M. No. 2872, British A.R.C., 1956.

16. Körner, H.: Untersuchungen zur Bestimmung der Druckverteilung a.. Flügel-Rumpf-Kombinationen - Teil I: MeBergebnisse für Mitteldeckeranordnung aus dem 1,3 m-Windkanal. DFVLR-Ber. Nr. 0562, 1969.

17. Labrujere, Th. E.; Loeve, W.; and Slooff, J. W.: An Approximate Method for the Calculation of the Pressure Distribution on Wing-Body Combinations at Subcritical Speeds. Aerodynamic Interference, AGARD CP No. 71, Jan. 1971, pp. 11-1 - 11-15.

18. Hess, John L.: Calculation of Potential Flow About Arbitrary Three-Dimensional Lifting Bodies. Rep. No. MDC J5679-01 (Contract N00019-71-C-0524), McDonnell Douglas Corp., Oct. 1972.

19. Paulson, John W.: Applications of Vortex-Lattice Theory to Preliminary Aerodynamic Design. Vortex-Lattice Utilization, NASA SP-405, 1976. (Paper no. 7 of this compilation.)

20. Tulinius, J. R.; and Margason, Richard J.: Aircraft Aerodynamic Design and Evaluation Methods. AIAA Paper No. 76-15, Jan. 1976.

21. Tulinius, J.: Theoretical Prediction of Wing-Fuselage Aerodynamic Characteristics at Subsonic Speeds. Rep. No. NA-69-789, Los Angeles Div., North American Rockwell Corp., 1969.

22. Tulinius, J. R.: Theoretical Prediction of Thick Wing and Pylon-Fuselage-Fanpod-Nacelle Aerodynamic Characteristics at Subcritical Speeds - Part I: Theory and Results. NASA CR-137578, 1974.

23. Woodward, F. A.; Dvorak, F. A.; and Geller, E. W.: A Computer Program for Three-Dimensional Lifting Bodies in Subsonic Inviscid Flow. Rep. No. USAAMRDL-TR-74-18, U.S. Army, Apr. 1974. (Available from DDC as AD 782 202.)

24. Chen, Lee-Tzong, Suciu, Emil O.; and Morino, Luigi: A Finite Element Method for Potential Aerodynamics Around Complex Configurations. AIAA Paper No. 74-107, Jan.-Feb. 1974.

25. Ehlers, F. Edward; Johnson, Forrester T.; and Rubbert, Paul E.: Advanced Panel-Type Influence Coefficient Methods Applied to Subsonic and Supersonic Flows. Aerodynamic Analyses Requiring Advanced Computers, Part II, NASA SP-347, 1975, pp. 939-984.

26. Hess, John L.: The Use of Higher-Order Surface Singularity Distributions to Obtain Improved Potential Flow Solutions for Two-Dimensional Lifting Airfoils. Comput. Methods Appl. Mech. & Eng., vol. 5, no. 1, Jan. 1975, pp. 11-35.

27. Bristow, D. R.: A New Surface Singularity Approach for Multi-Element Airfoil Analysis and Design. AIAA Paper No. 76-20, Jan. 1976.

28. Mohn, L. W.: Comparison of Wind-Tunnel Test Results at $M_\infty = 0.7$ With Results From the Boeing TEA-230 Subsonic Flow Method. NASA CR-2554, 1975.

FLOW FIELD AT ANY POINT DUE TO AN ARBITRARY BODY IS GIVEN BY EQUIVALENCE RULE:

FLOW FIELD DUE TO ACTUAL BODY = SOLUTION FOR EQUIVALENT BODY OF REVOLUTION + 2-D SOLUTION FOR ACTUAL BODY CROSS-SECTION A-A - 2-D SOLUTION FOR EQUIVALENT CROSS-SECTION A-A

3-D BOUNDARY CONDITIONS ARE SATISFIED IN THESE 2-D SOLUTIONS

Figure 1.- General slender body theory.

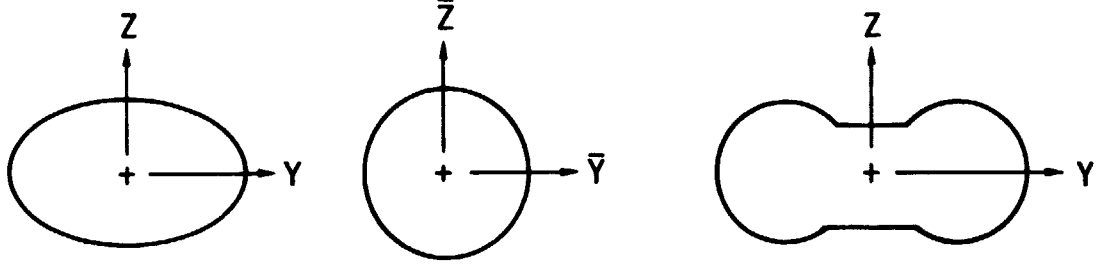

u-PLANE $\bar{u}$-PLANE

CONFORMAL TRANSFORMATION DISTRIBUTED SINGULARITIES

Figure 2.- Methods for solving two-dimensional cross-flow potential for arbitrary cross sections.

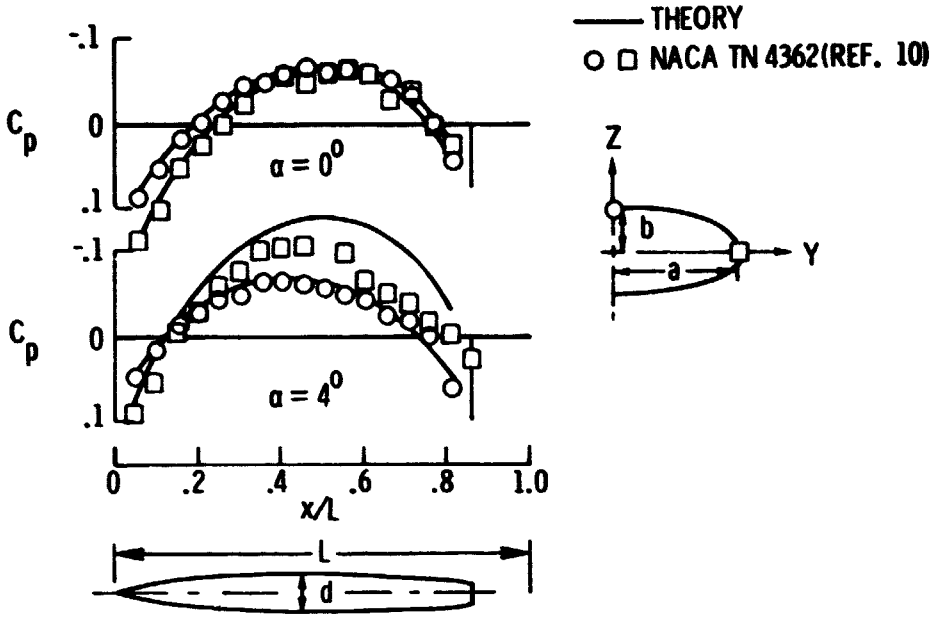

Figure 3.- Comparison of slender body theory and experiment. $L/d = 12$; $M_\infty = 0.9$; $a/b = 3$.

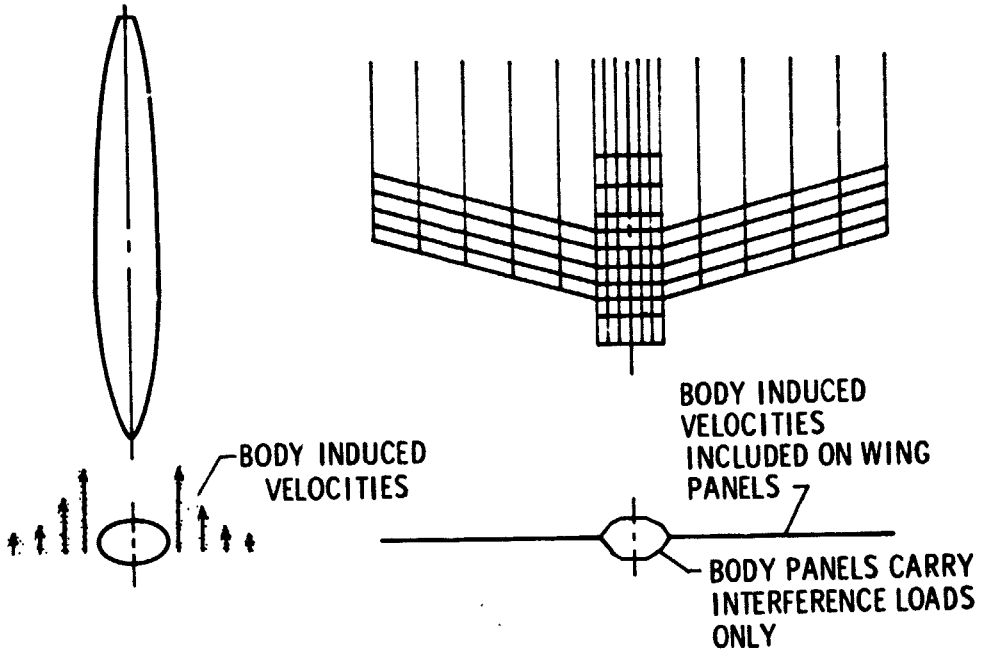

Figure 4.- Schematic of utilization of general slender body in vortex-lattice theory.

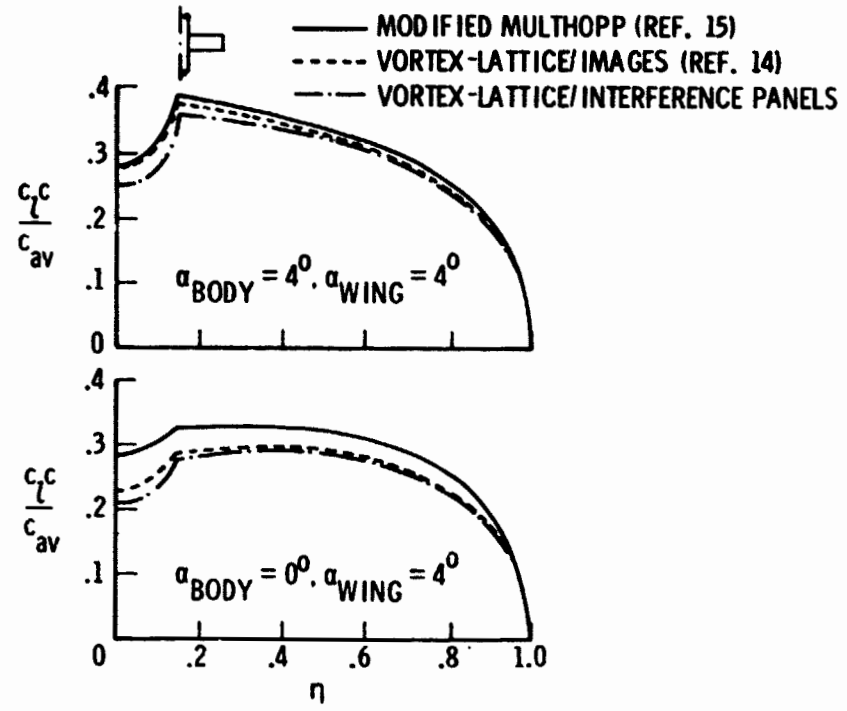

Figure 5.- Spanwise load calculation for wing-body combination. M_∞ =0; A = 5; d/c = 0.72; Λ = 0; λ = 1.

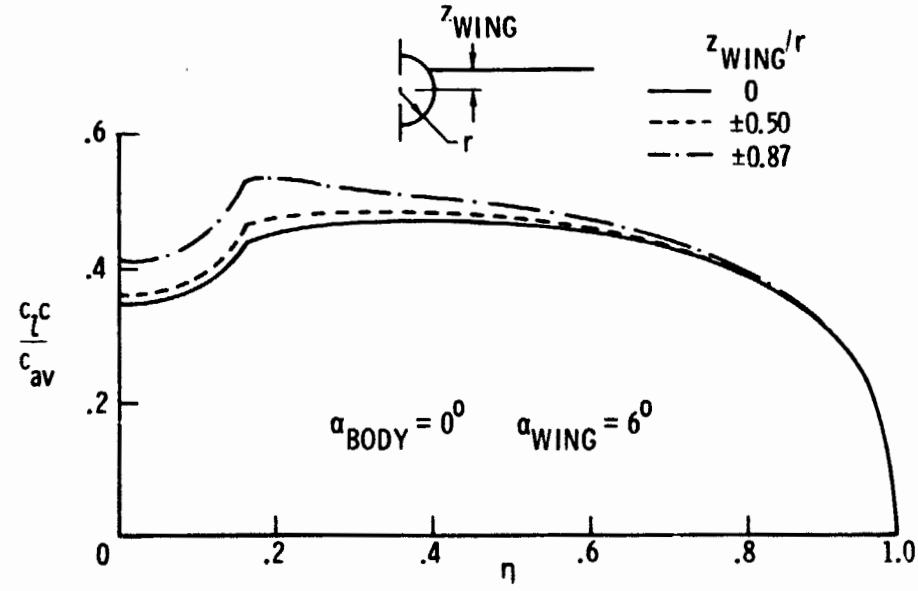

Figure 6.- Variation of wing placement for A = 6 wing and infinite circular-cylinder combination using vortex lattice with interference paneling. M_∞ = 0; d/c = 1; Λ = 0; λ = 1.

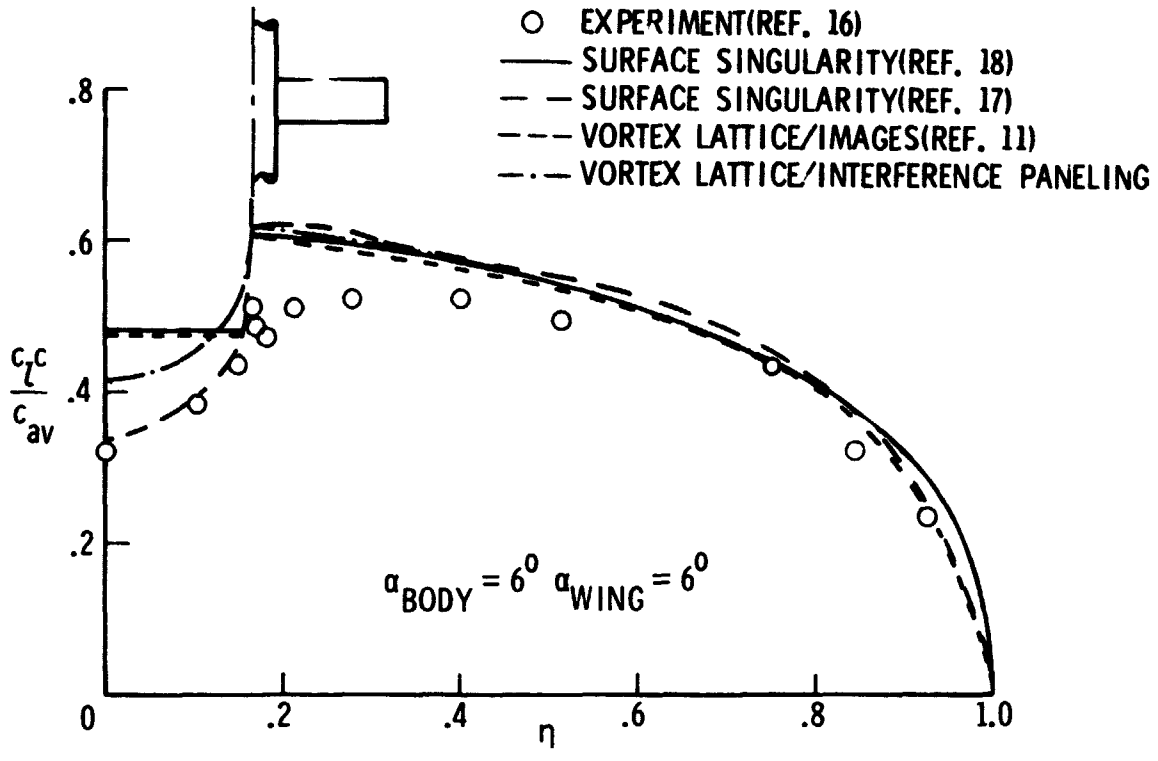

Figure 7.- Comparison of theory and experiment for A = 6 wing and infinite circular-cylinder combination. RAE 101 section; $M_\infty = 0$; d/c = 1; $\Lambda = 0$; $\lambda = 1$.

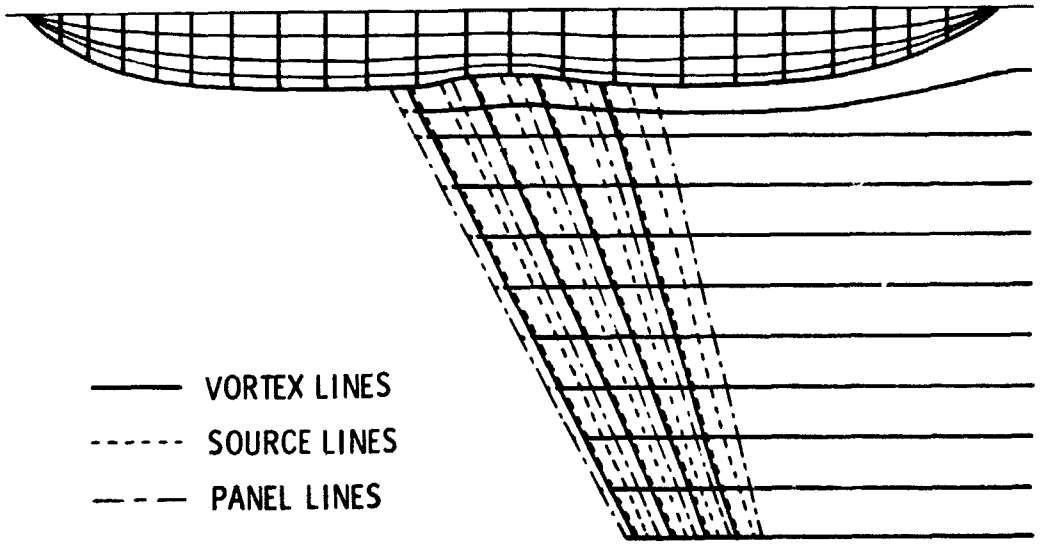

Figure 8.- Quadrilateral vortex and source lattice analysis and design.

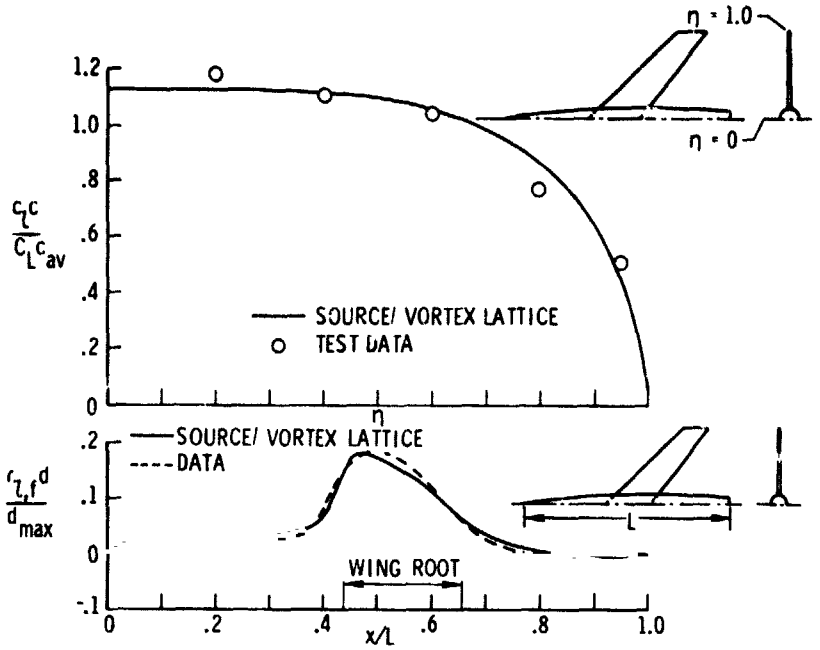

Figure 9.- Quadrilateral vortex and source lattice results for a wing-body combination. $M_\infty = 0.6$; $\alpha = 4^o$.

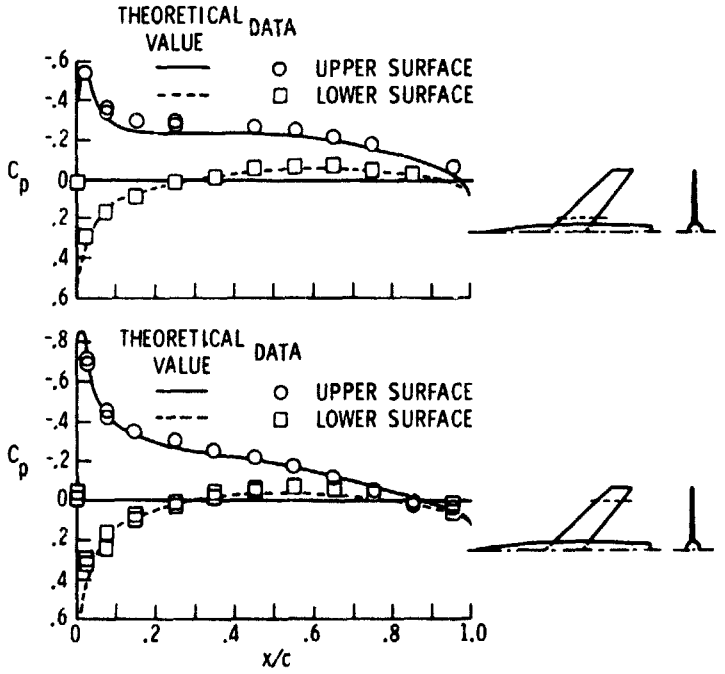

Figure 10.- Quadrilateral vortex and source lattice wing-surface pressure coefficients. $M_\infty = 0.6$; $\alpha = 4^o$.

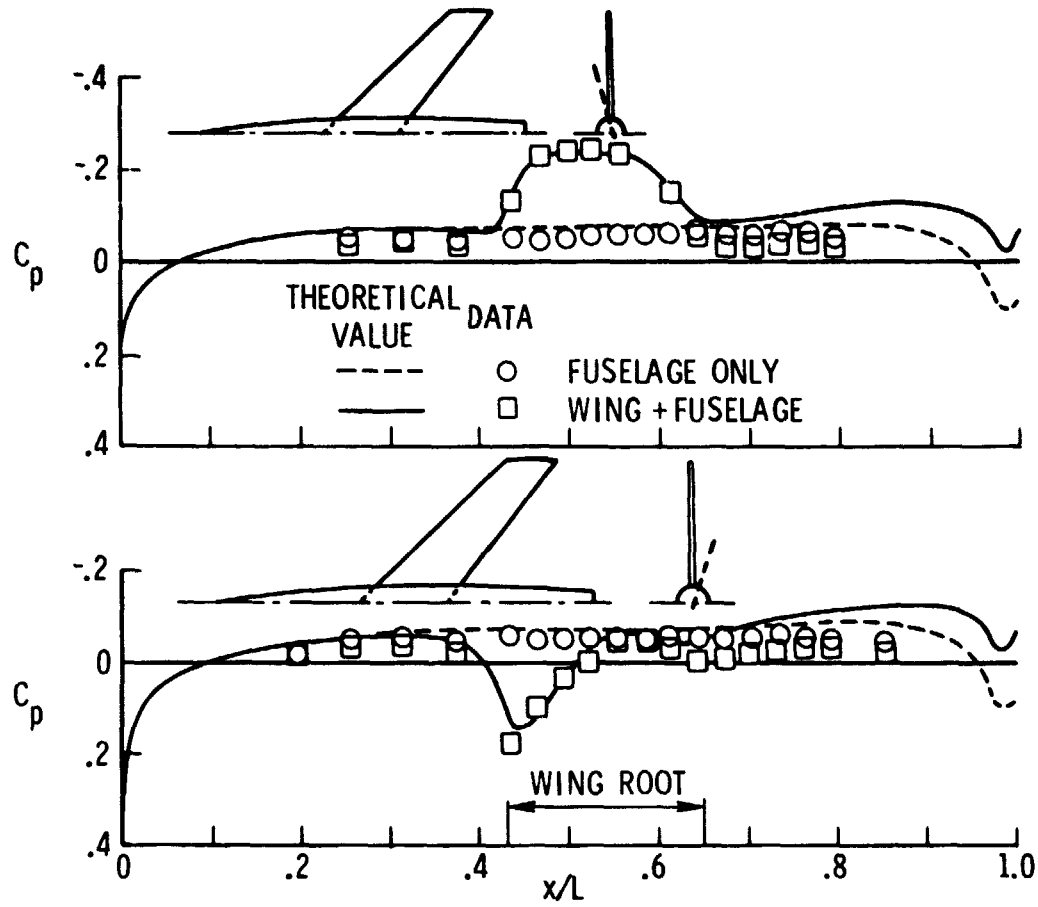

Figure 11.- Quadrilateral vortex and source lattice body-surface pressure coefficients. $M_\infty = 0.6$; $\alpha = 4^o$.

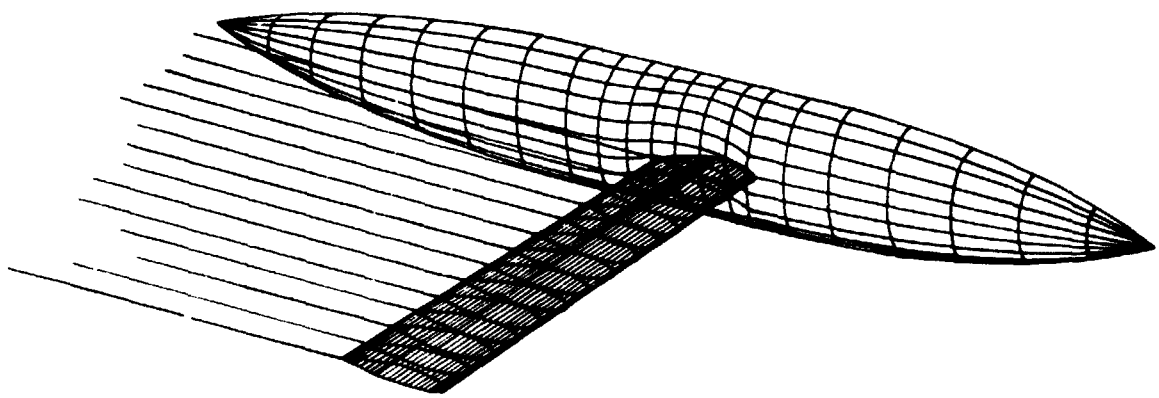

Figure 12.- Representative paneling for three-dimensional surface singularity approach.

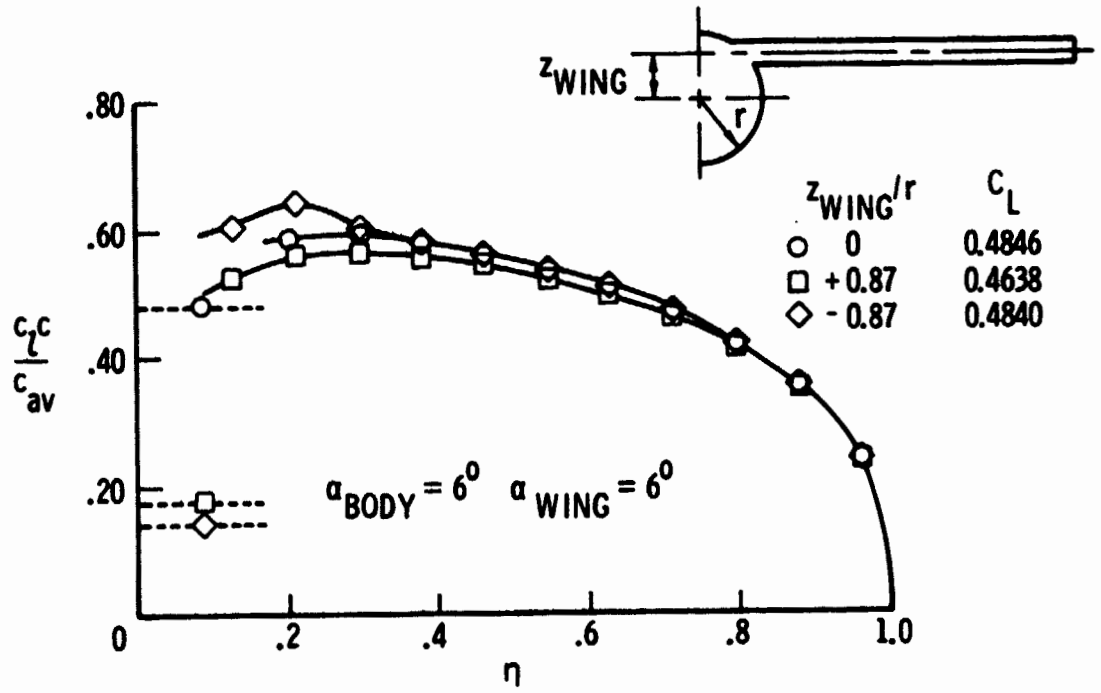

Figure 13.- Variation of wing placement for A = 6 wing and infinite circular-cylinder combination using Hess surface singularity approach (ref. 18). RAE 101 section (thickness = 0.09c); $M_\infty = 0$; d/c = 1; $\Lambda = 0$; $\lambda = 1$.